Radiative models for rapid blazar flares

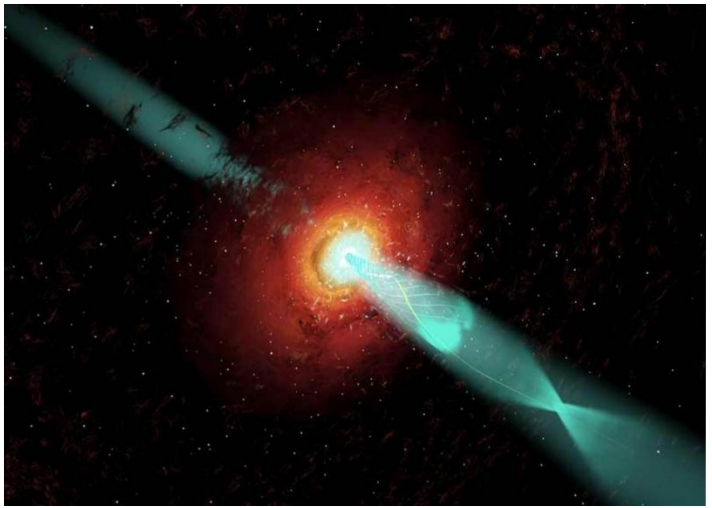

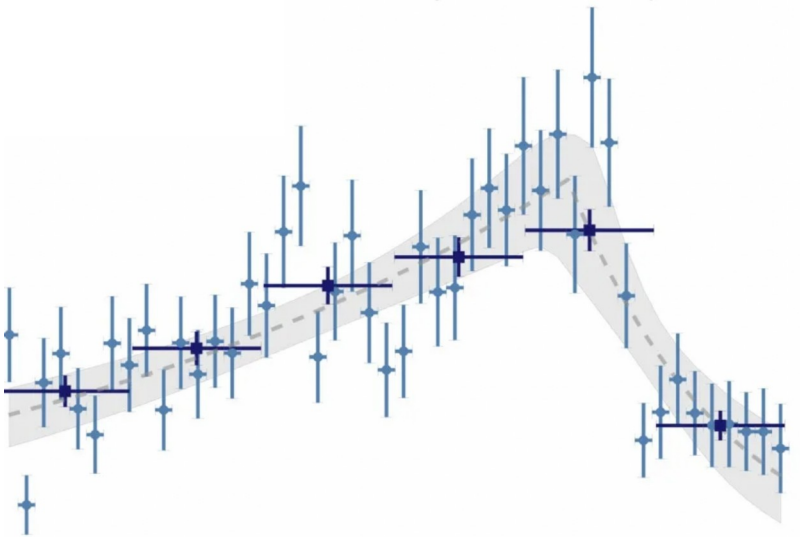

A. Zech

PHNE theory meeting 2024

LUTH Observatoire de Paris | PSL

blazar emission in the leptonic model

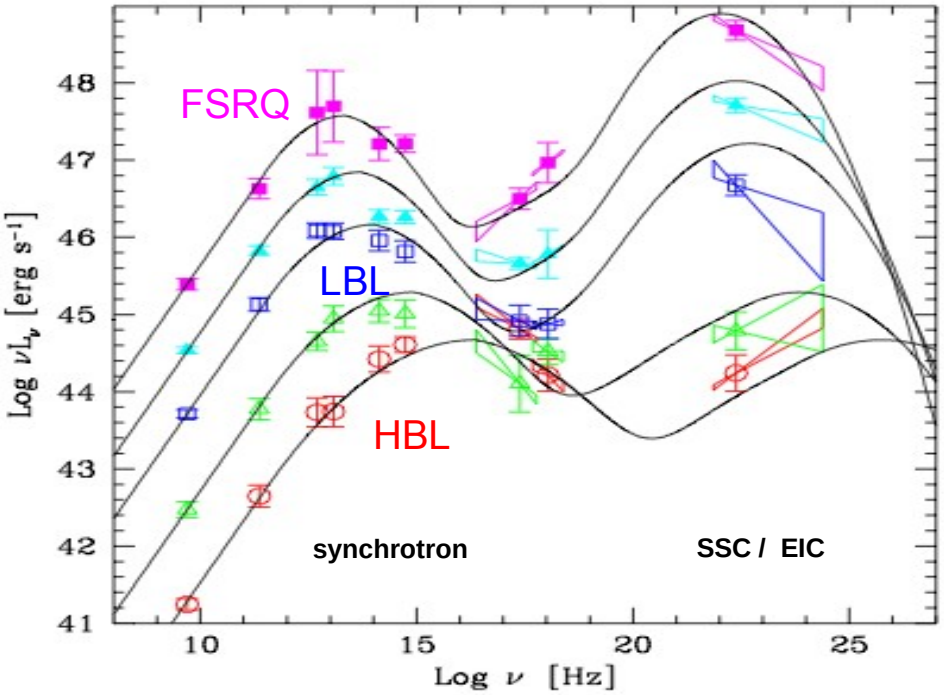

Donato et al. (2002), based on Fossati et al. (1998)

luminous **FSRQs** with high peaks in gamma band ↔ less luminous **BL Lac objects** with lower peaks in gamma band

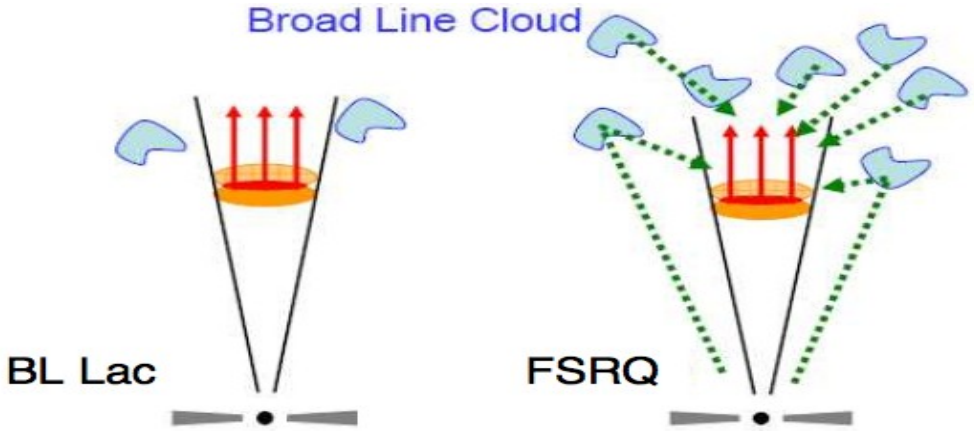

B. Lott, Cospar 02/10

- Disk and Broad Line Region emit weakly

- γ-rays due to **Synchrotron Self Compton**

- Disk and Broad Line Region emit strongly

- γ-rays mostly due to **External Inverse Compton** → high Compton dominance

physical origin of flares

1) variation of the macroscopic parameters of the emission region

- change in size of emission region R → particle density, magnetic field B (expansion, contraction)

- change in magnetic field B or external radiation field

- change in Doppler beaming (Lorentz factor, viewing angle)

2) variation in the energy distribution of the emitting particles

- particle injection (pre-accelerated particle distribution)

- particle acceleration (shock, turbulence, shear, magnetic reconnection)

variation of the parameters of the emission region

a case study

(work with S. Le Bihan, A. Dmytriiev 2024;
cf. Proceedings of Gamma 2024 Conf.)

an orphan flare from 3C 279 in 2013 ?

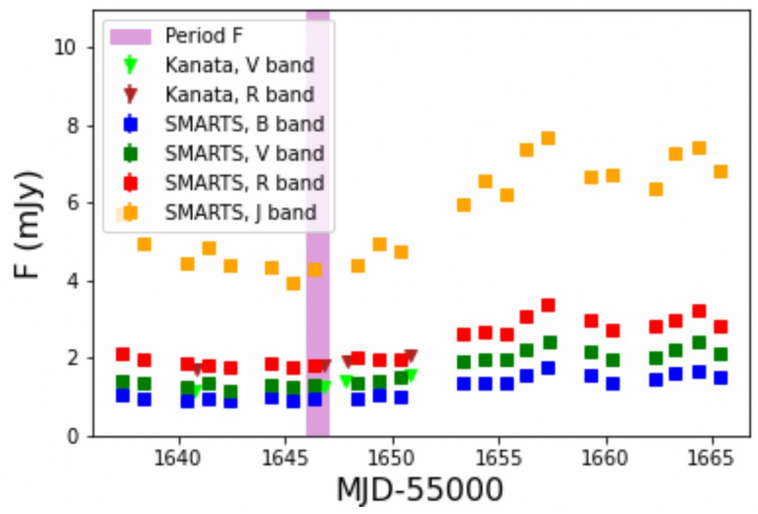

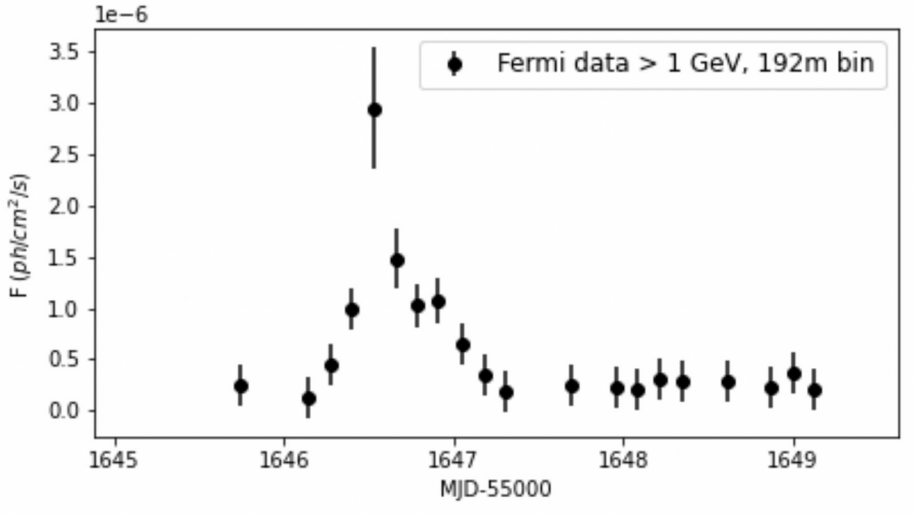

Bihan 2024;
with data from Hayashida et al. 2015

- significant Fermi flare from this FSRQ on 20.12.2013
- no significant variability in simultaneous optical data
- no simultaneous X-ray data

the model : low state

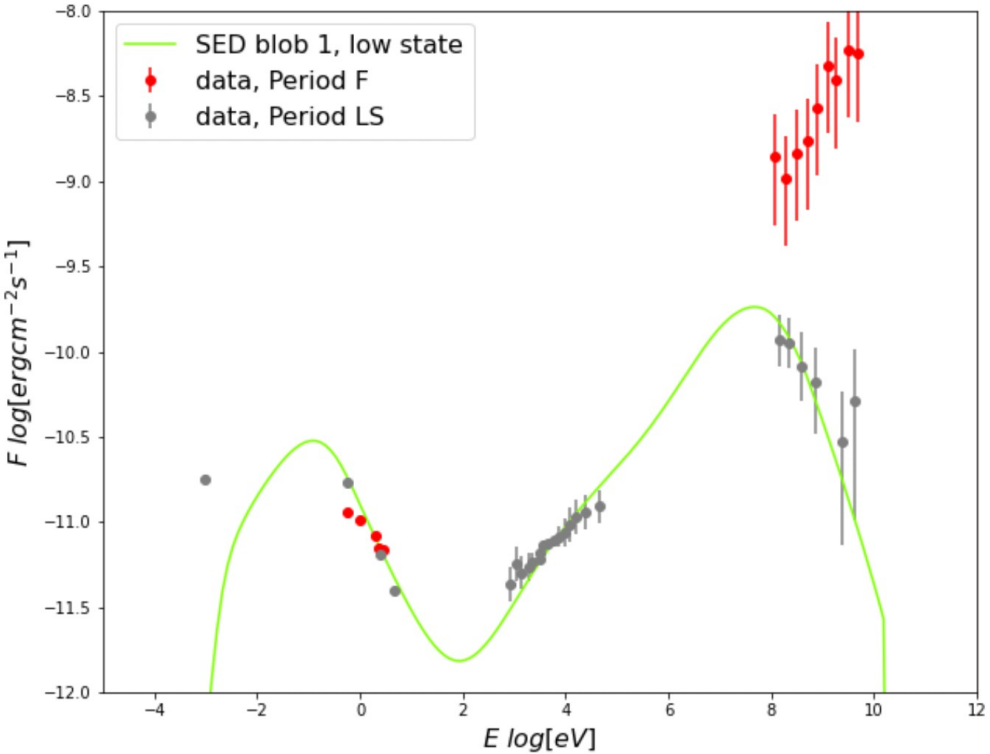

- time-dependent leptonic model EMBLEM including external photon fields (disk, BLR, dust torus)

- continuous emission during low state modelled with single stationary emission region (“blob 1”)

- steady-state spectrum from injection of a steep power-law + cooling + particle escape

- B’ = 2.5 G , Doppler factor ~ 19 , $R'_{blob1} \sim 2 \times 10^{16}$ cm , distance from black hole : $d_1 \sim 5 \times 10^{16}$ cm

the model : BLR

- External Compton emission dominated by the photon field from the Broad Line Region

- photons from a spectrum of emission lines

- BLR modelled as a spherical shell with inner radius $R_{BLR} \sim 3 \times 10^{17}$ cm (0.1 pc)

- For distance d > R_{BLR}, the energy density decreases as :

$$U'(\epsilon', d) = \frac{L'_{BLR}(\epsilon')\Gamma^2_{blob}}{3\pi R^2_{BLR} c\left(1+\left(d/R_{BLR}\right)^{\beta_{BLR}}\right)}$$

(Hayashida et al 2012)

- index β_{BLR} set to 4

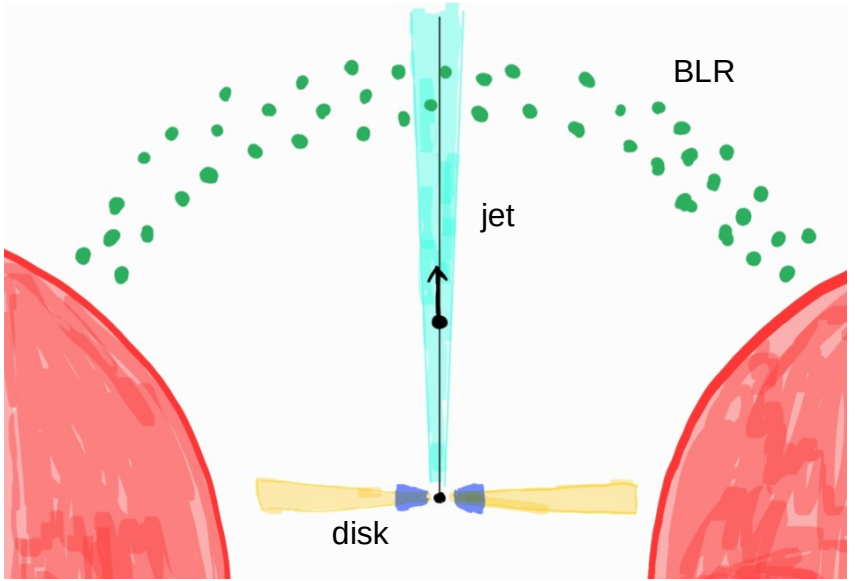

the model : accelerating blob

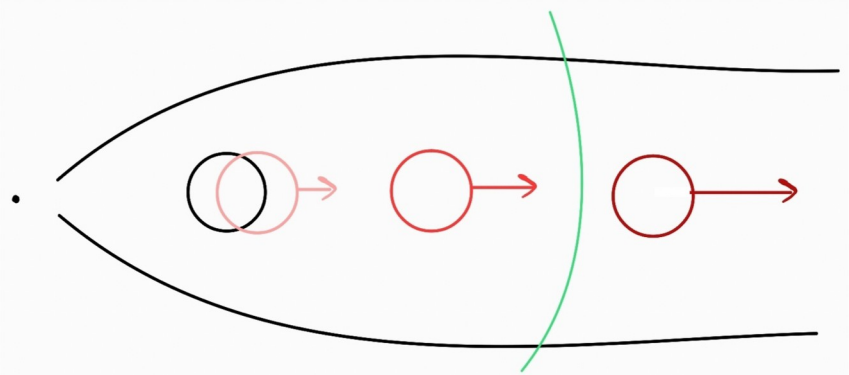

flare is caused by an accelerating, expanding emission region (“blob 2”) (differential collimation) :

$$\Gamma_{blob} = min\left(\Gamma_{max}, \sqrt{d/(3R_s)}\right)$$

(Ghisellini & Tavecchio 2009)

$\Gamma_{max} = 30$

acceleration up to $d_{max} = 4 \times 10^{17}$ cm

- for $d < R_{BLR}$, as blob 2 accelerates :

$$U' \propto d$$

- for $d > d_{max}$, as blob 2 advances at constant velocity :

$$U' \propto d^{-\beta_{BLR}}$$

- particle spectrum from injection of a steep power-law + cooling (incl. adiabatic) + particle escape

- initial B’ = 0.01 G , initial $R'_{blob2} \sim 2 \times 10^{16}$ cm

model vs. data

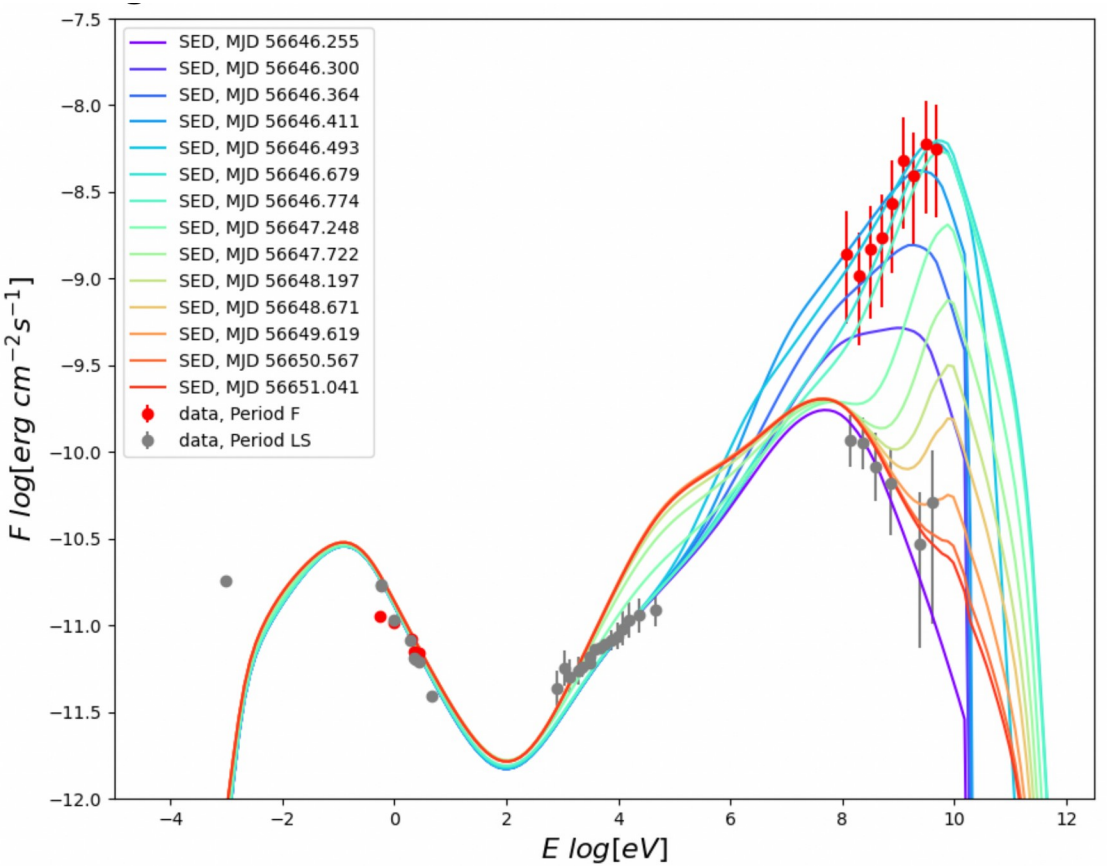

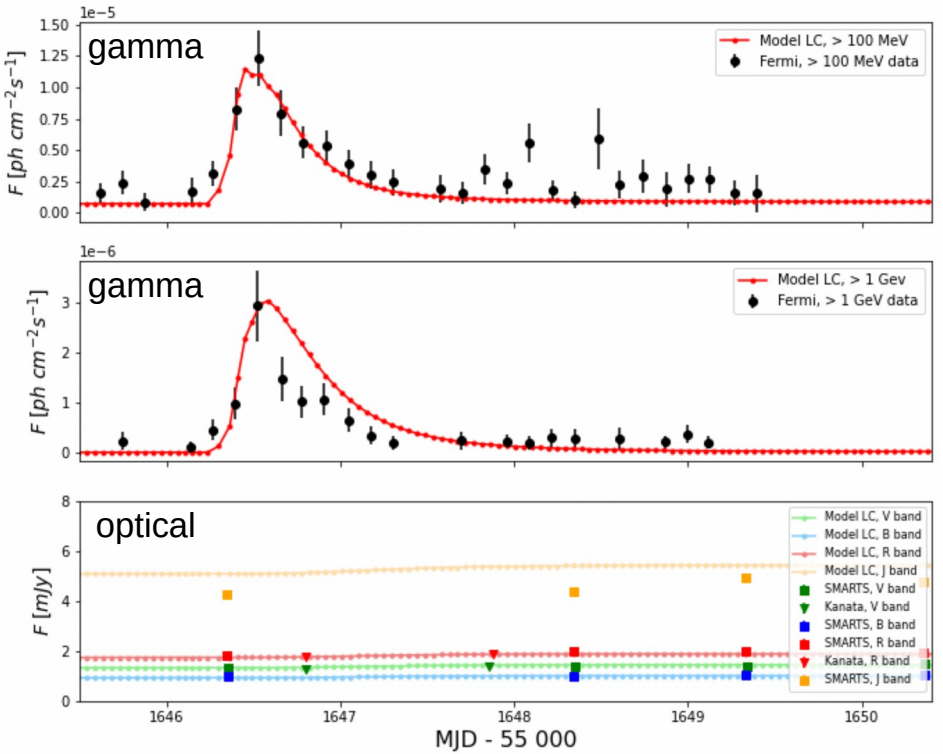

first conclusions

The good overall agreement between model and data suggests that our scenario of an accelerating blob can explain orphan flares from FSRQs without any variation of the particle distribution.

In this scenario, the **flare decrease** reflects the **BLR density profile**.

Issues with our parameters requiring further scrutiny :

- large difference between the magnetic field strengths assumed for blob1 and blob2

- modelling of stationary blob1 not entirely self consistent

variation of the particle distribution

a systematic study

(work with P. Thevenet, C. Boisson, A. Dmytriiev 2023/2024; publication to be submitted)

particle evolution in the EMBLEM code

Cooling terms — Acceleration terms

$$\frac{\partial N_e(\gamma,t)}{\partial t} = \frac{\partial}{\partial \gamma}\left[\left(b_c(\gamma,t)\gamma^2 + \frac{1}{t_{ad}}\gamma - a(t)\gamma - \frac{2}{\gamma}D_{F_{II}}(\gamma,t)\right)N_e(\gamma,t)\right] + \frac{\partial}{\partial \gamma}\left(D_{F_{II}}(\gamma,t)\frac{\partial N_e(\gamma,t)}{\partial \gamma}\right)$$
$$- N_e(\gamma,t)\left(\frac{1}{t_{esc}} + \frac{3}{t_{ad}}\right) + \dot{Q}_{inj}(\gamma,t)$$

Injection term

Cooling

- Synchrotron and Inverse Compton: $b_c(\gamma,t)$
- Adiabatic expansion: $t_{ad}(t) = \frac{R(t)}{\beta_{exp} c}$
- Escape: $t_{esc}^{(turb)} = \left(\frac{R}{c}\right)^2 \left(\frac{\delta B}{B}\right)^2 \frac{c}{\lambda_{max}} \left(\frac{r_L}{\lambda_{max}}\right)^{q-2}$

Acceleration

- Fermi I: $a = 1/t_{shock}$, $\dot{Q}(\gamma,t)$
- Fermi II: $D_{F_{II}}(\gamma,t) = \frac{p^2}{t_{F_{II}}}$

$$t_{F_{II}} = \frac{1}{\beta_A^2}\left(\frac{\delta B}{B}\right)^{-2} \frac{\lambda_{max}}{c}\left(\frac{r_L}{\lambda_{max}}\right)^{2-q}$$

the scenarios

injection

Q_{inj} : fixed injection rate, fixed PL spectrum, injected during flare window

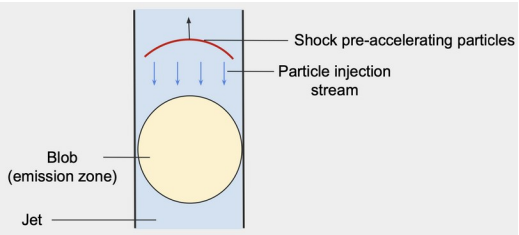

Fermi-I acceleration

Q_{inj} with increasing γ_{max} during flare window
t_{FI} : time-scale of γ_{max} evolution

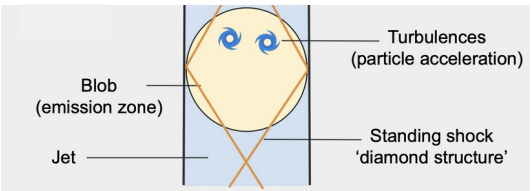

Fermi-I re-acceleration

Q_{inj} : fixed continuous PL injection
t_{shock} : time-scale for sys. energy gain

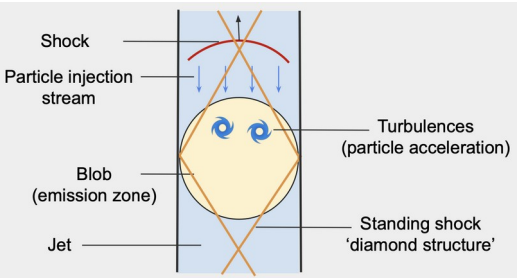

injection & adiabatic expansion

Q_{inj} plus fixed expansion rate

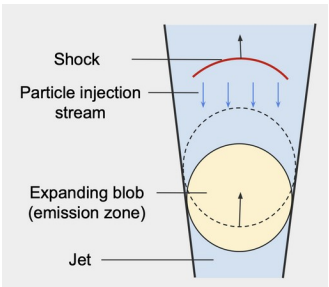

Fermi-II acceleration

injection of cold particles
t_{FII} : acceleration time scale

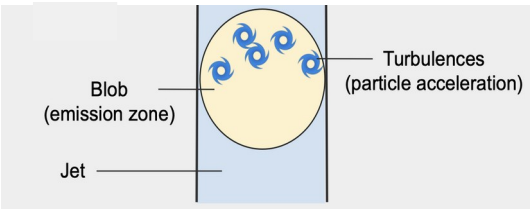

Fermi-II re-acceleration

Q_{inj} : fixed continuous PL injection
t_{FII} : acceleration time-scale

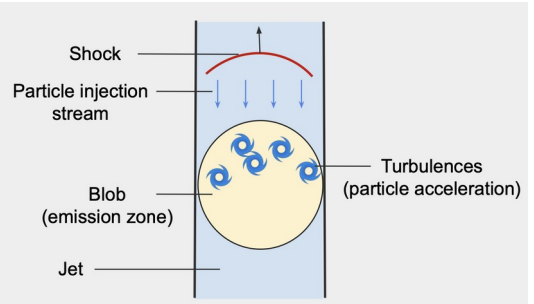

example : Fermi-I acceleration

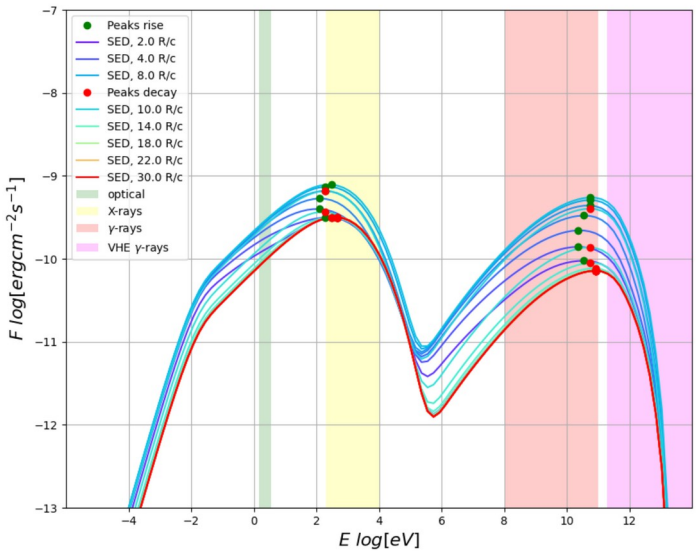

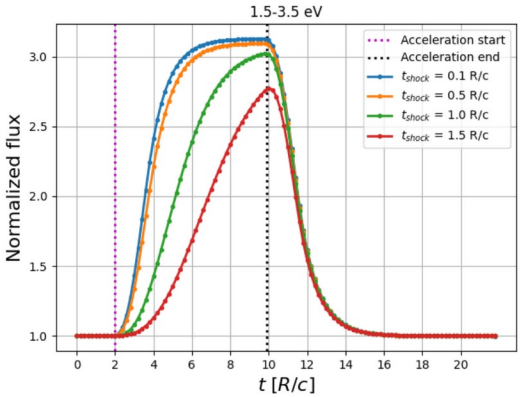

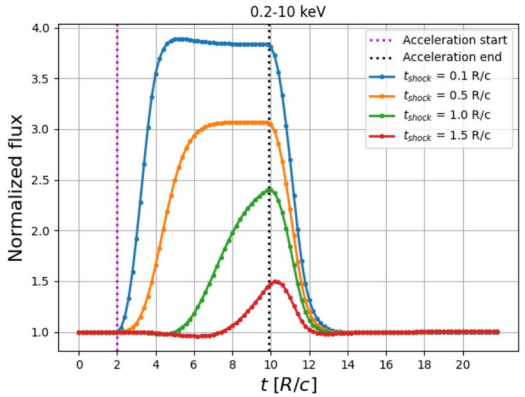

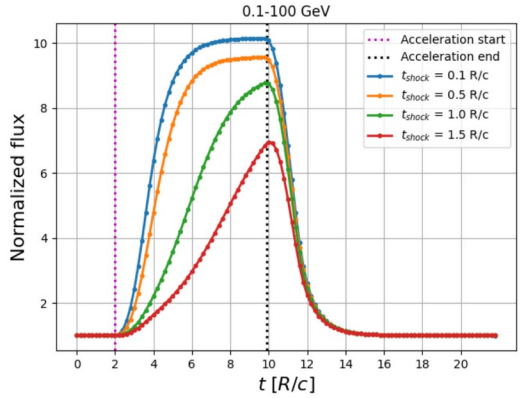

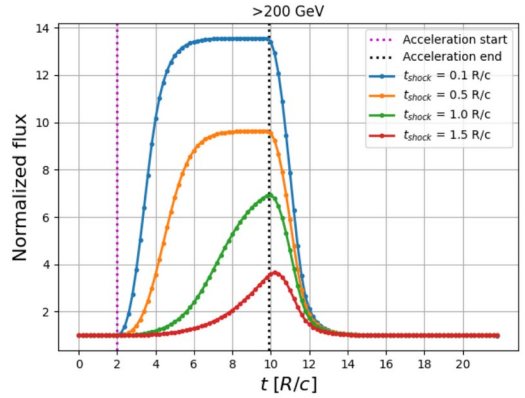

- shift of peaks during flare

- flare onset shifts between energy bands

- occurrence of a “plateau” in light curves only for very rapid t_{shock}

example: Fermi-II re-acceleration

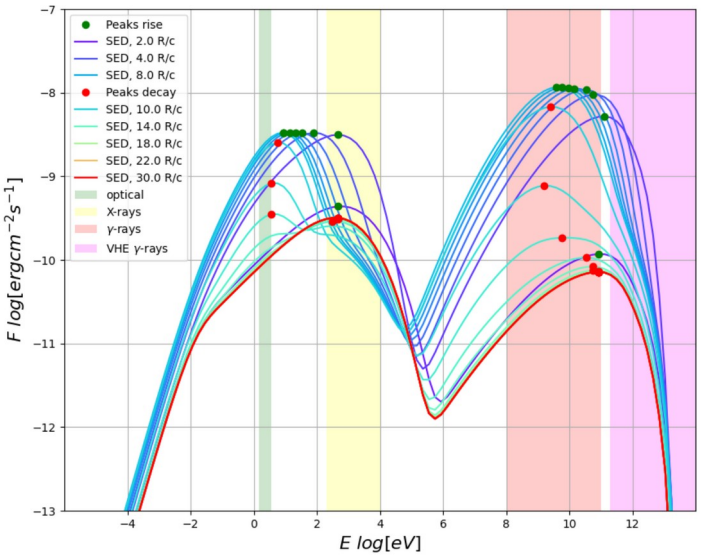

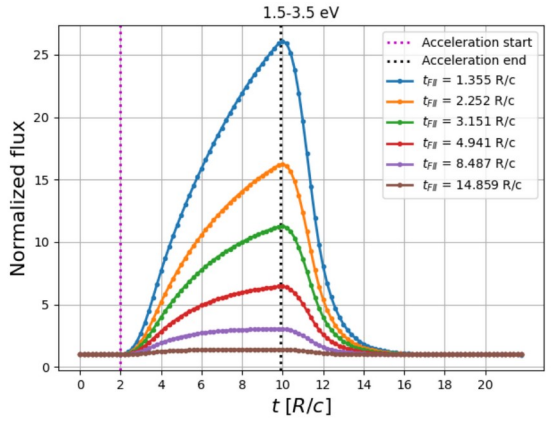

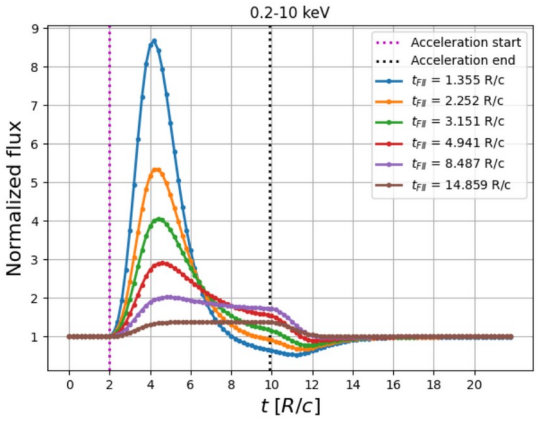

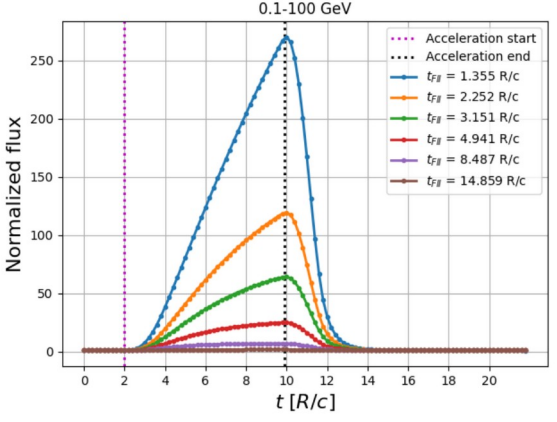

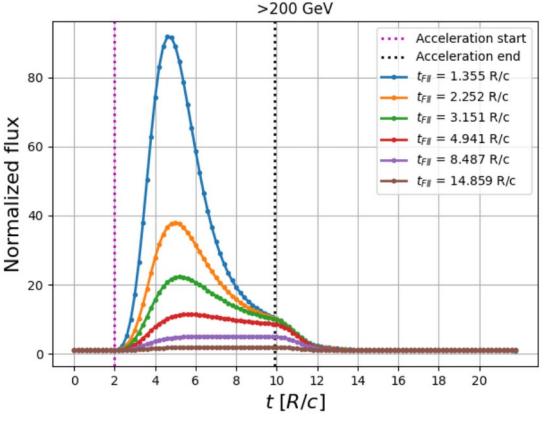

- strong shift of peaks during flare
  → hysteresis

- Compton dominance > 1 for very rapid t_{FII}

- strong energy dependant time delays between light curves for very rapid t_{FII}

light-curve comparison

Even for a single emission region, a large variety of flare shapes !

• **injection** scenarios : onset of the flare rise occurs at the same time in all bands. Occurence of plateaux.

• **Fermi-I** scenarios : flare onset is delayed at higher energies.

• **Fermi-II** scenarios : flare onset occurs ~ at the same time in different bands. Acceleration of cold particles does not reach a plateau. Efficient re-acceleration leads to a flare that is peaking earlier at higher energies.

Decay times determined by the escape time and the effect of radiative cooling.

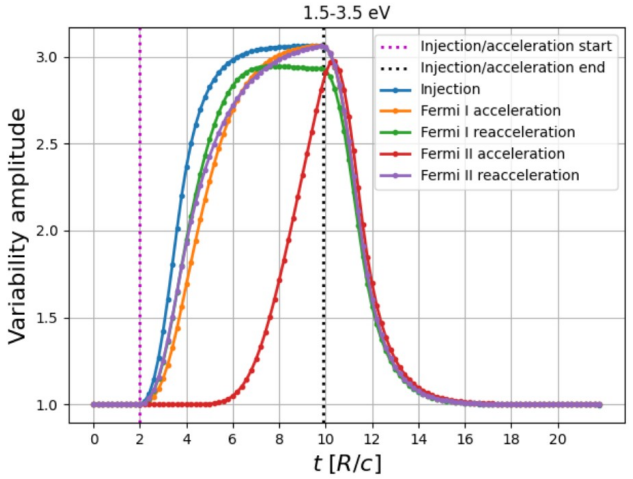

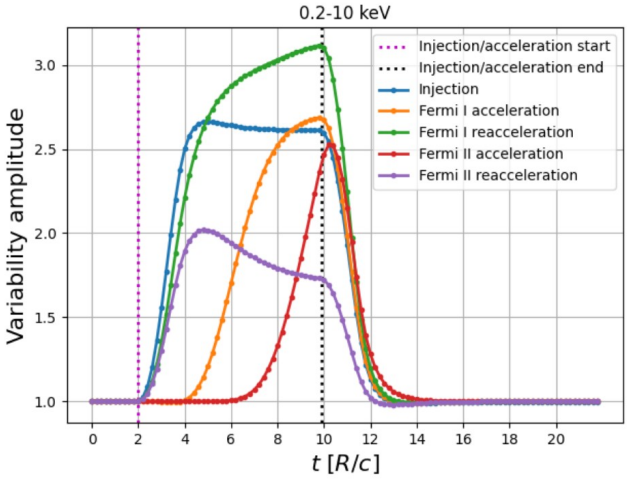

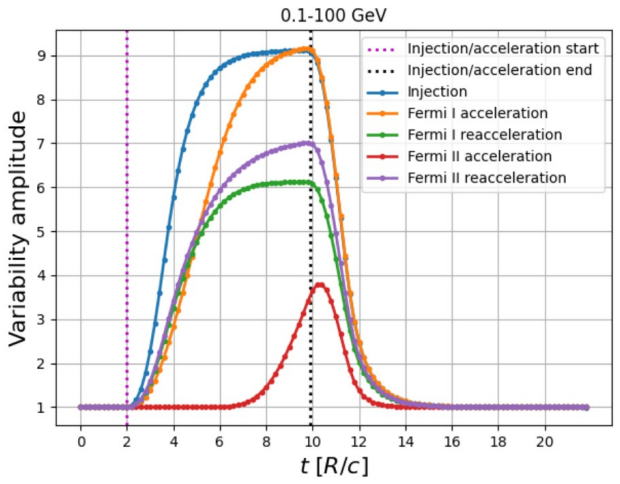

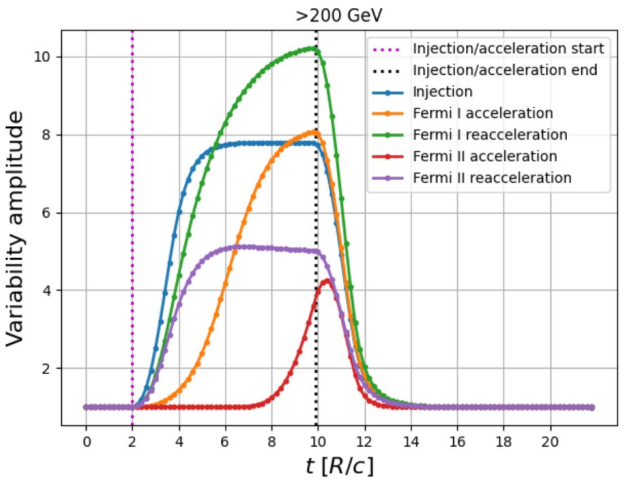

application to a flare of Mrk 421

First application to a 2013 flare from Mrk 421 (BL Lac object) to illustrate the light-curve shapes of different scenarios :

- none of the generic scenarios provides a satisfactory representation of the data
  → very difficult to get the fluxes right between energy bands without fine-tuning injection rate and spectral index

- time delays of the peak flux can appear even between neighbouring energy bands

→ a full representation of SED and light curves might require a combination of scenarios & automated fitting procedure

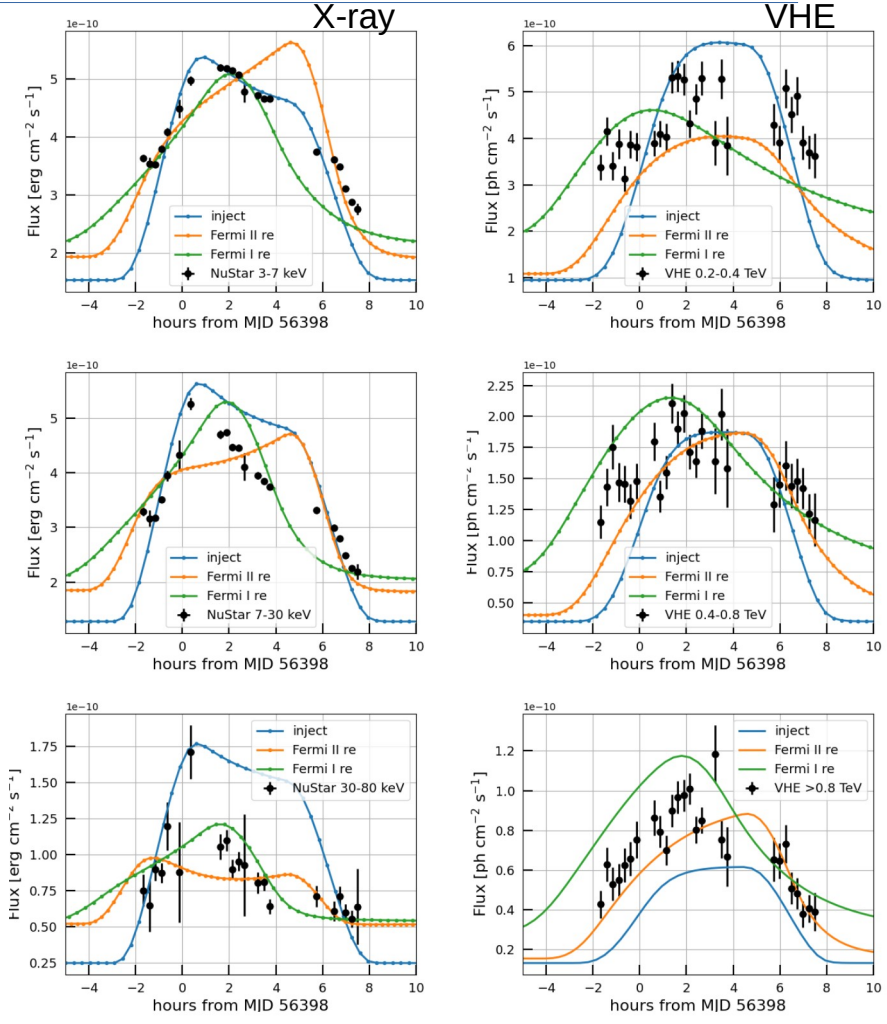

Conclusions

Blazar flares can arise from a **variety of physical processes**.

In addition to statistical studies (power spectrum densities, structure functions, fractional variability…), it is important to **identify specific signatures** for a given physical cause.

Comparison with data is not trivial. Well sampled MWL flare data are needed on the one hand and models covering different basic and more evolved scenarios on the other.

backup

injection & adiabatic expansion

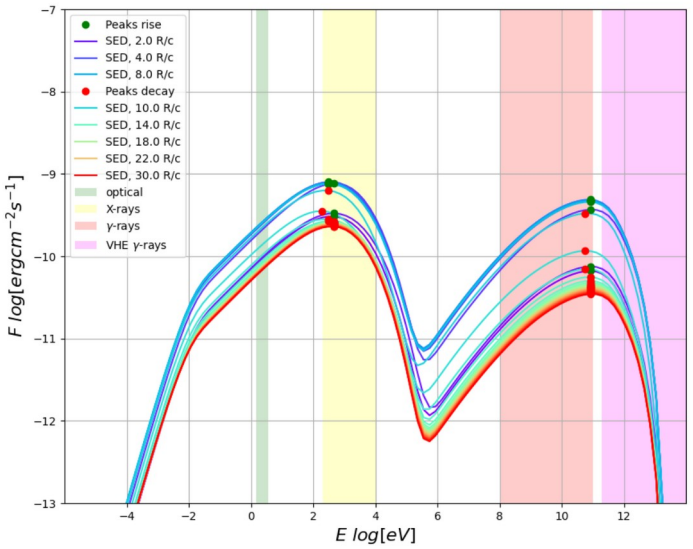

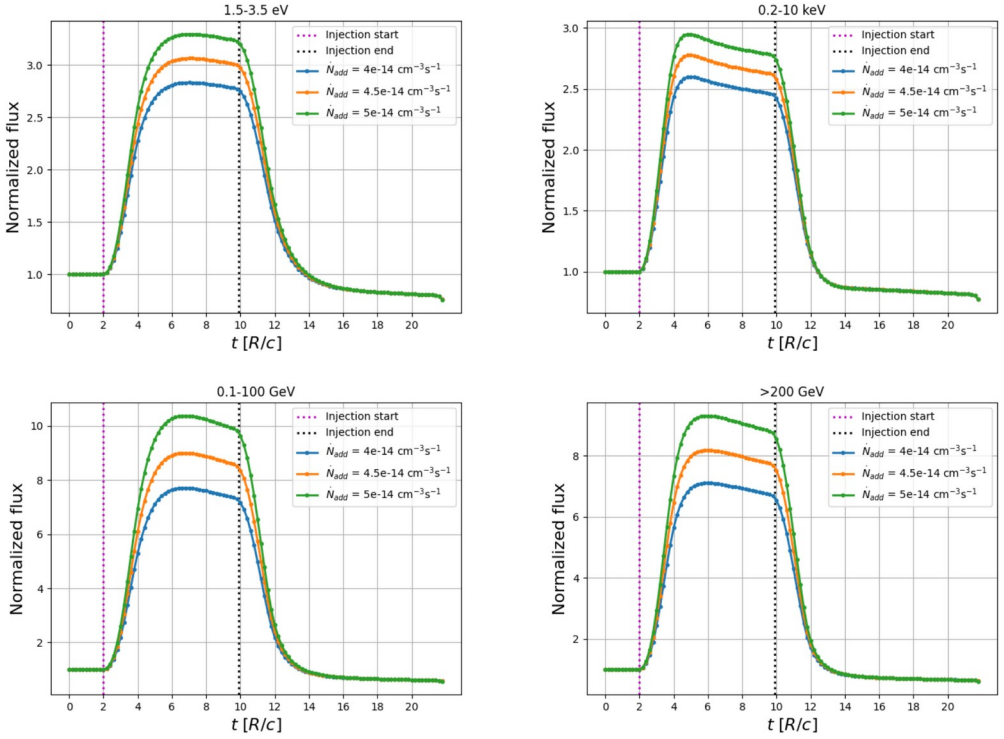

Fermi-II acceleration

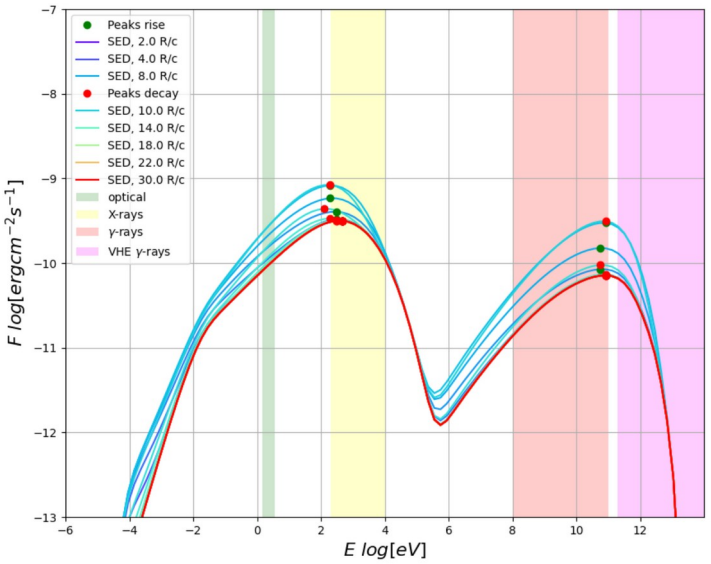

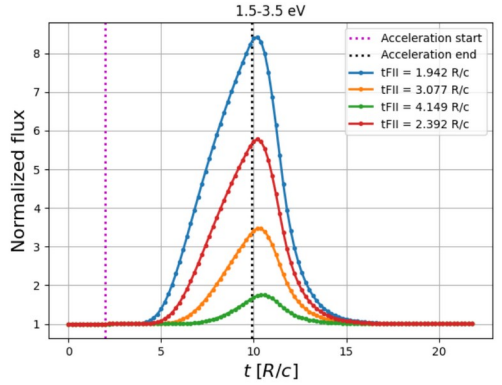

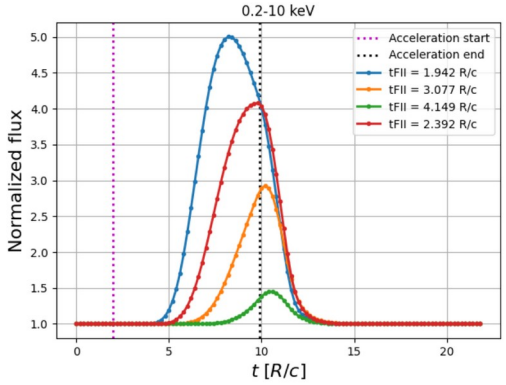

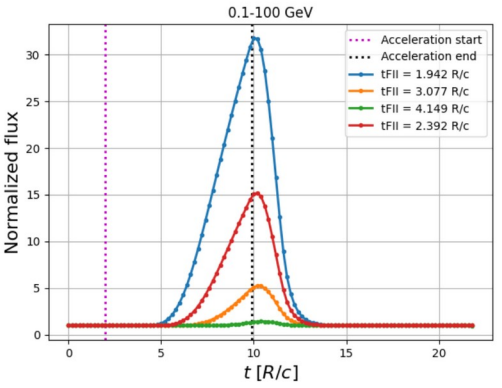

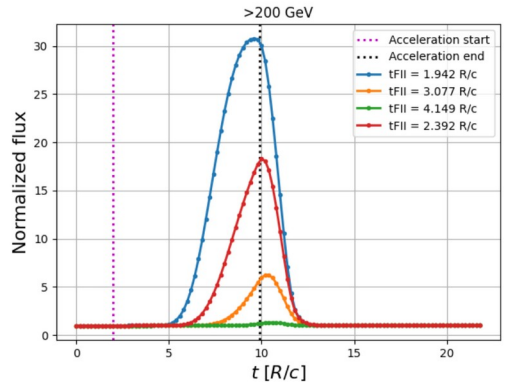

Fermi-I re-acceleration

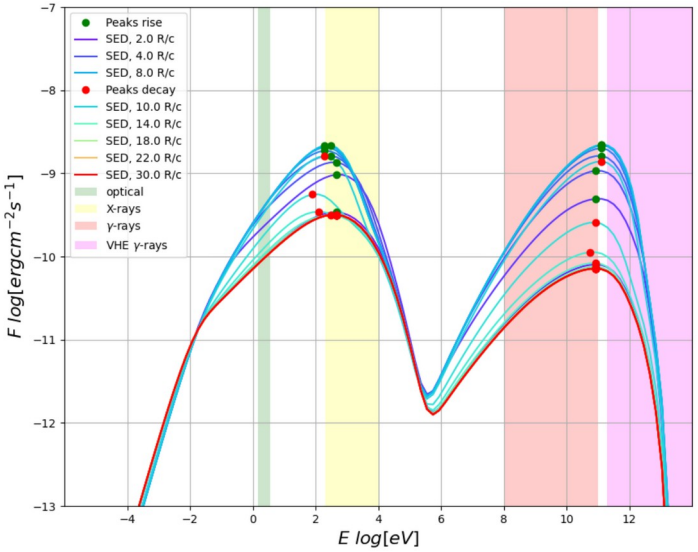

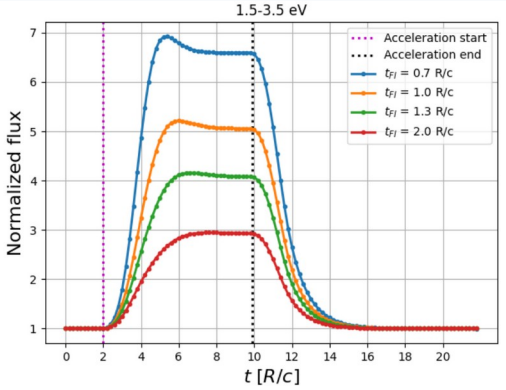

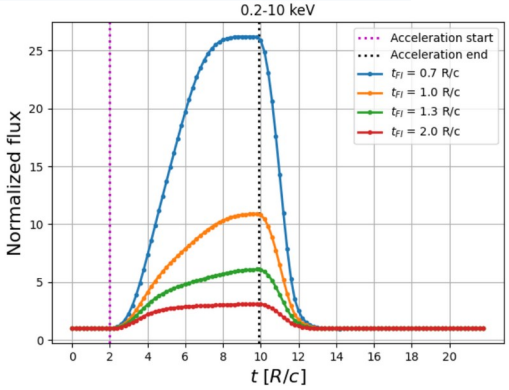

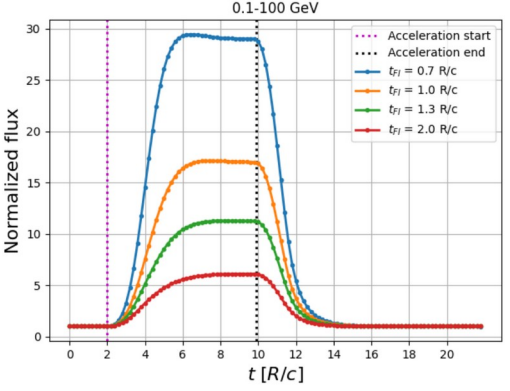

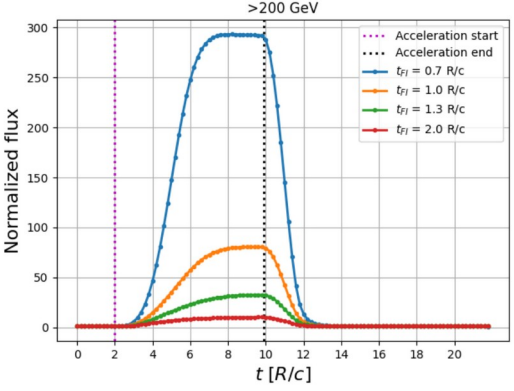

model parameters

	Blob characteristics	Injection spectrum
Blob 1	**Type** : stationary **Magnetic field** $= 2.5\ G$ $R_{b-BH} = 0.5 \times 10^{17}\ cm$ $R_b = 2.1 \times 10^{16}\ cm$	**Type** : PL $\mathbf{N} = 3.0 \times 10^{-4} cm^{-3} s^{-1}$ $\gamma_{pivot} = 215$ $\alpha_{inj} = -3.5$ $\gamma_{min} = 675$ $\gamma_{max} = 10^7$
Blob 2	**Type** = accelerating **Magnetic field** $= [0.01, 0.0086]\ G$ $R_{b-BH} = [0.1, 50] \times 10^{17}\ cm$ $R_b = [2.4, 2.8] \times 10^{16}\ cm$	**Type** = PL $\mathbf{N} = 2.5 \times 10^{-4} cm^{-3} s^{-1}$ $\gamma_{pivot} = 200$ $\alpha_{inj} = -3.5$ $\gamma_{min} = 1300$ $\gamma_{max} = 10^7$

Redshift	$z = 0.536$
Initial Doppler factor	$\delta_i = 18.8$
Final Doppler factor	$\delta_f = 30$
Jet angle	$\theta_j = 1.91°$
Black hole mass	$M_{BH} = 1.0 \times 10^{42}$ g $= 0.5 \times 10^9\ M_\odot$
Disk luminosity	$L_d = 1.0 \times 10^{46}$ erg/s
BLR fraction	$f_{BLR} = 0.1$
BLR power law index	$\beta_{BLR} = 4$
DT fraction	$f_{DT} = 0.1$
DT temperature	$T_{DT} = 1500$ K

particle acceleration in jets

Possibly there is no single mechanism at play, but several mechanisms contribute in different regions of the jet.

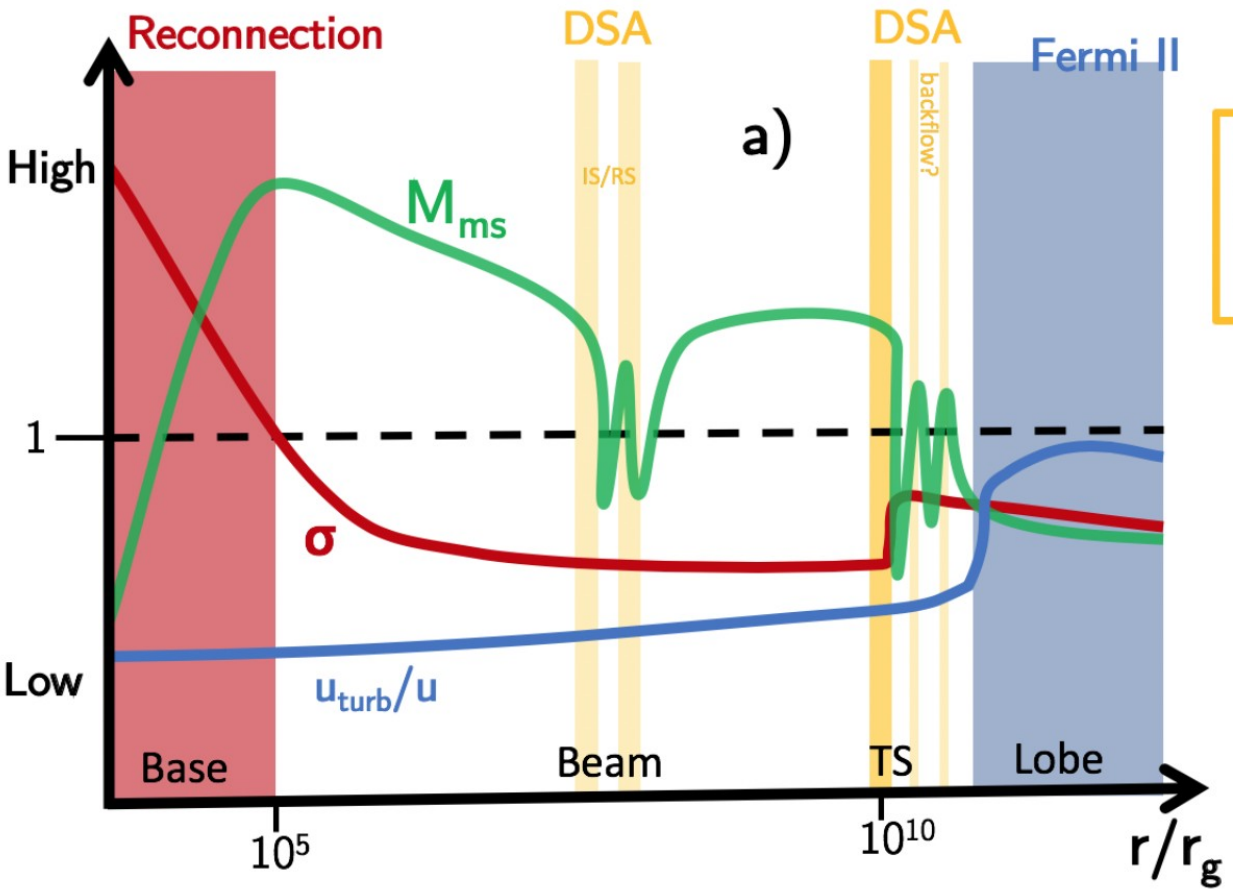

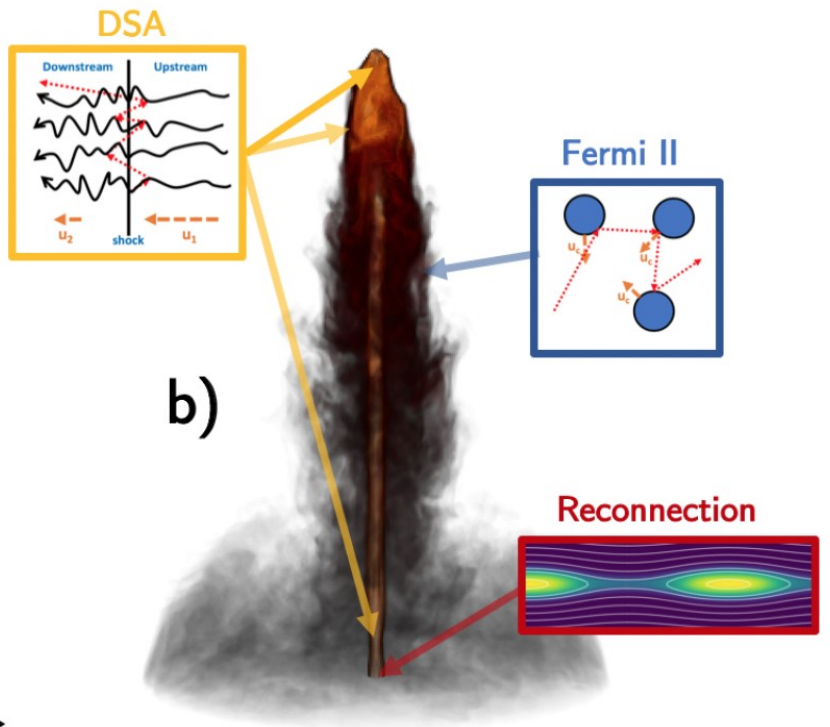

Matthews, Bell, Blundell 2020

an example : modelling a flare from Mrk 421

In this model, the continuous low-state emission from Mrk 421 is connected with a flare in Feb. 2010 :

- low state is modelled with a continuous injection (+ cooling, escape) of electrons accelerated on a (bow) shock into the emitting blob

- the hard spectrum during the flare requires additional Fermi II acceleration from a turbulent emission region surrounding the blob as it passes through an inhomogeneous region inside the jet.

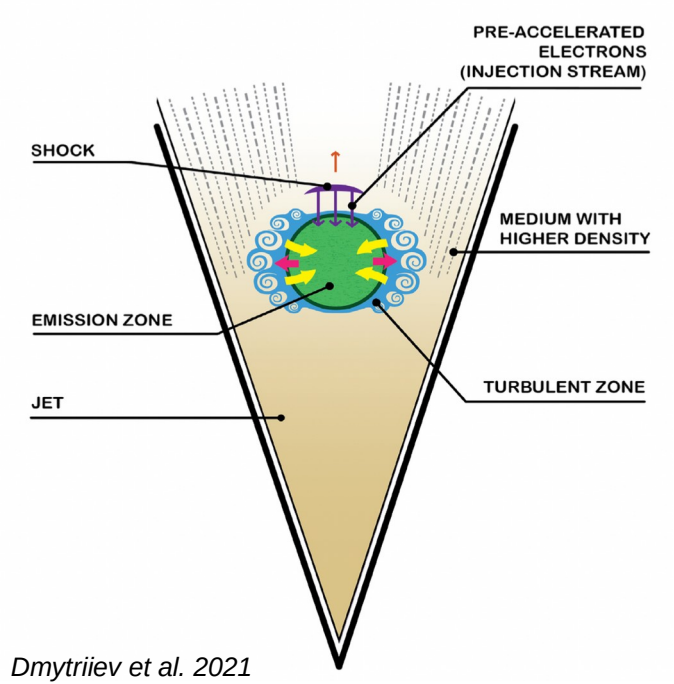

A. Dmytriiev et al. 2021

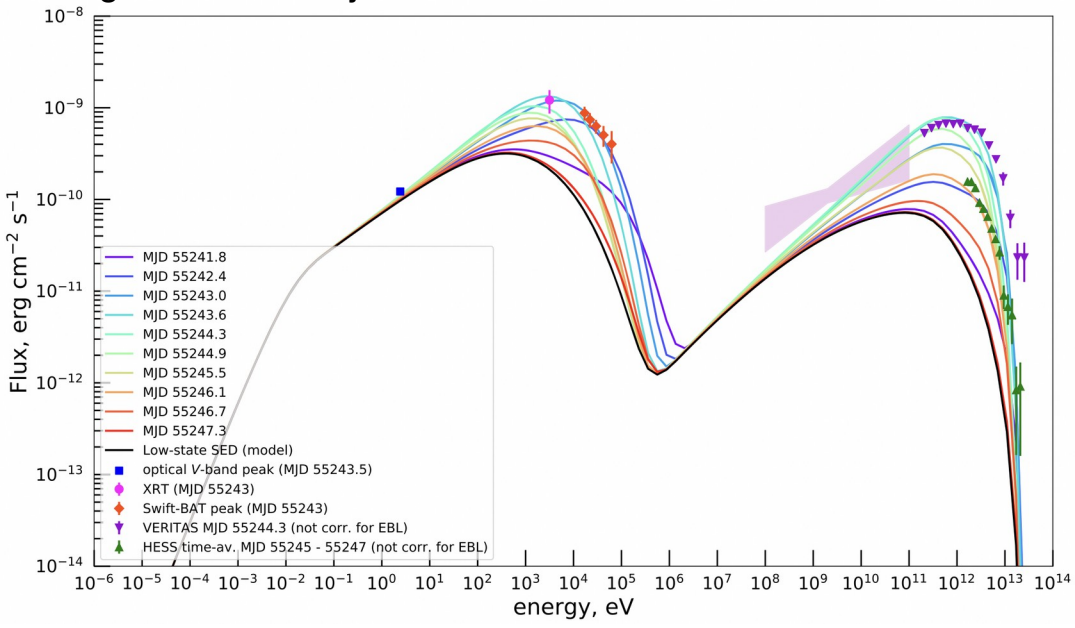

Broad-band emission from Mrk 421 during low state and flare + model curves. (*A. Dmytriiev et al. 2021)*

an orphan flare from 3C 279 in 2013 ?

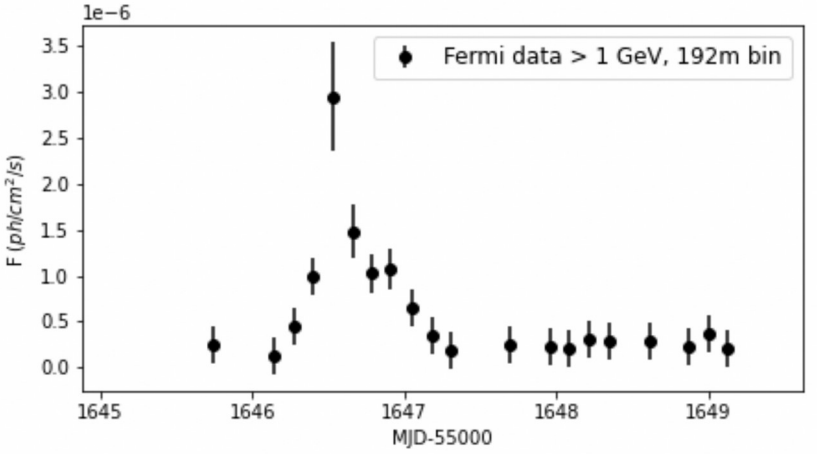

Le Bihan 2024;
with data from Hayashida et al. 2015

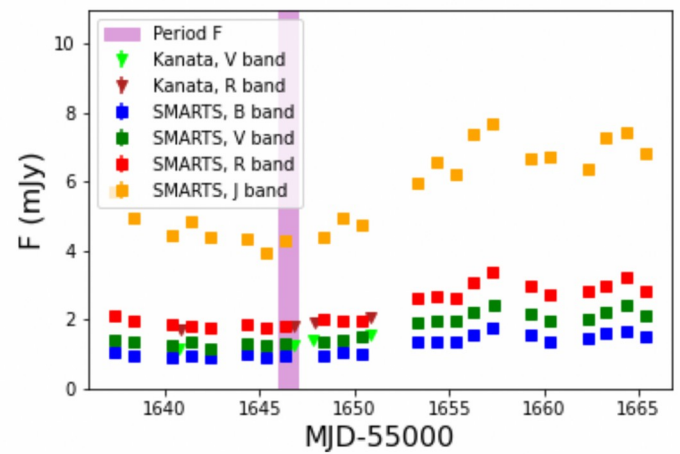

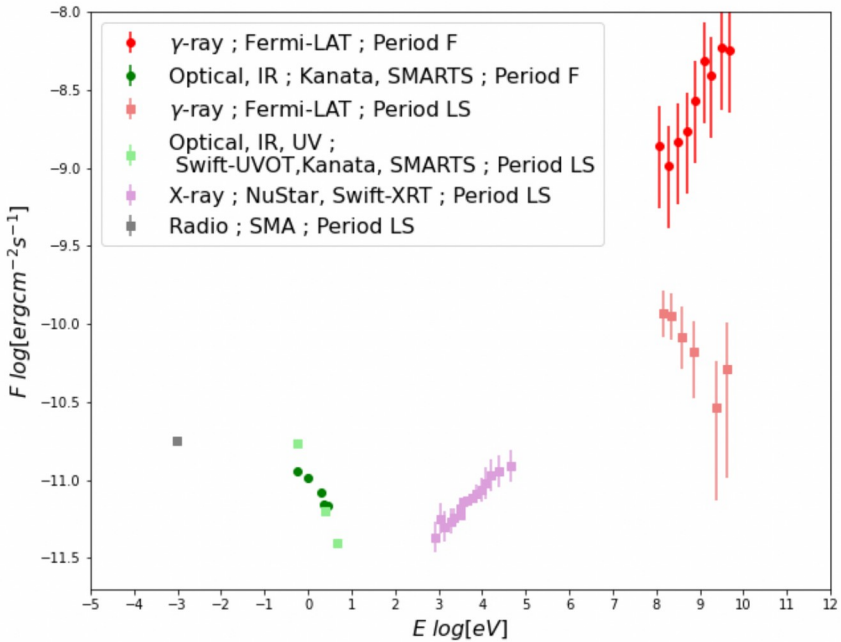

- significant Fermi flare from this FSRQ on 20.12.2013
- no significant variability in simultaneous optical data
- no simultaneous X-ray data

origin of flares in the one-zone model

example: flare through injection, radiative cooling, escape

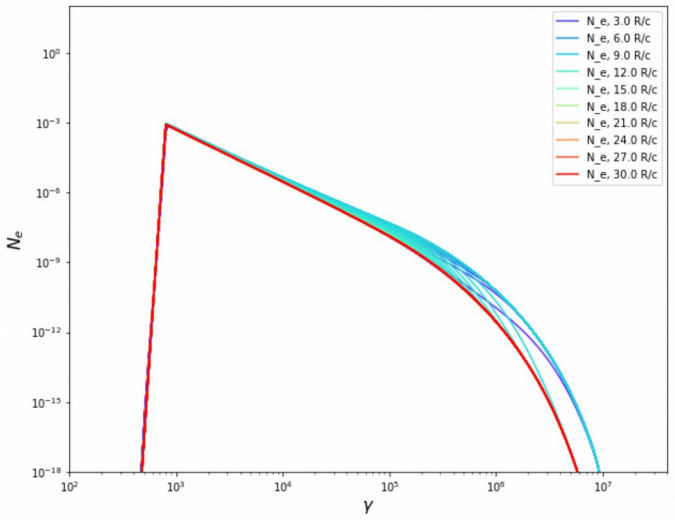

e- distribution : steady state (violet) + injection, radiative cooling, escape

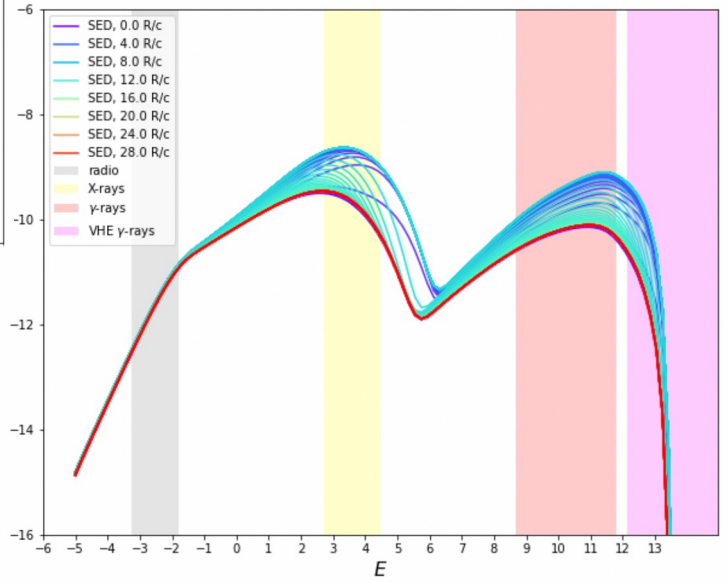

Spectral Energy Distribution

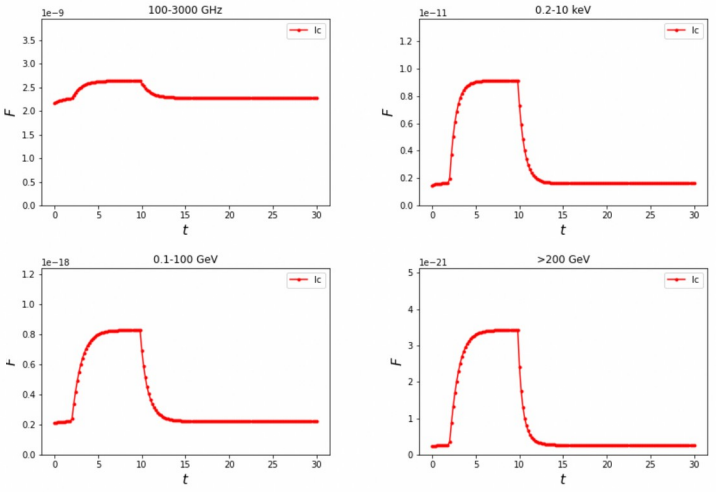

Light curves

P. Thevenet, internship, 2023

the VLBI – high-energy connection

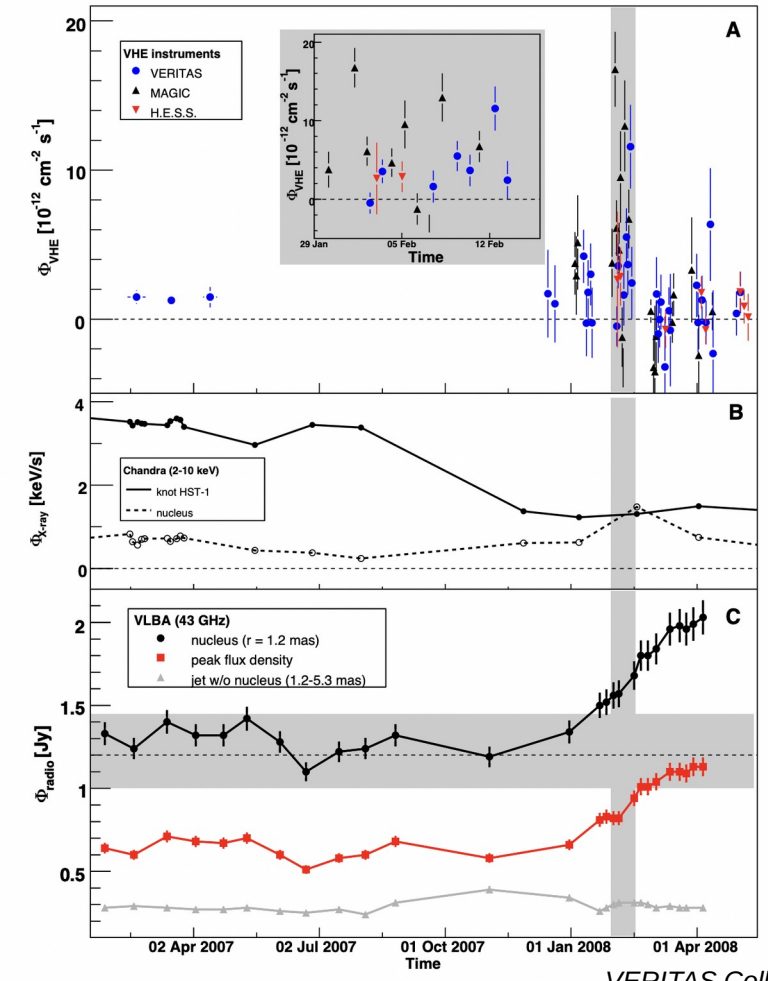

VERITAS Collab. et al. 2009

2008 VHE flare of the radio galaxy M87 :

Correlation with high activity
(radio VLBI, X-rays) from the nucleus
(radio core).

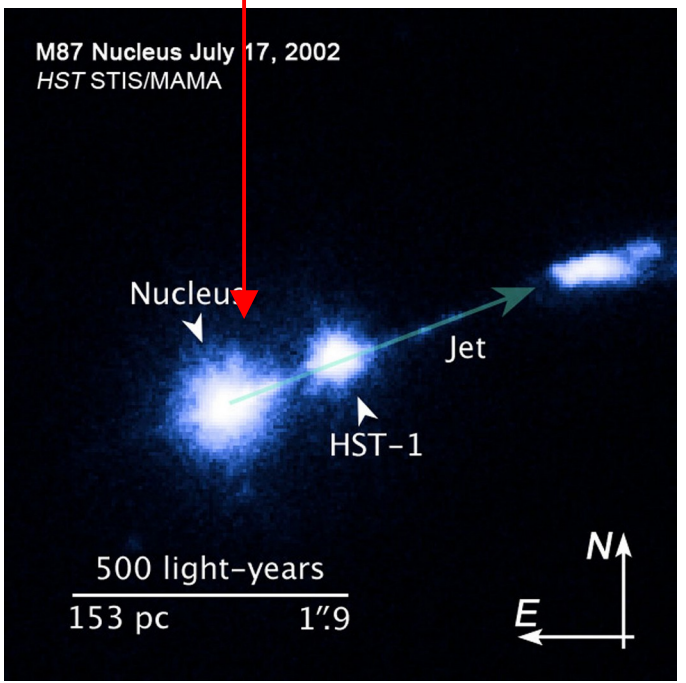

the VLBI – high-energy connection

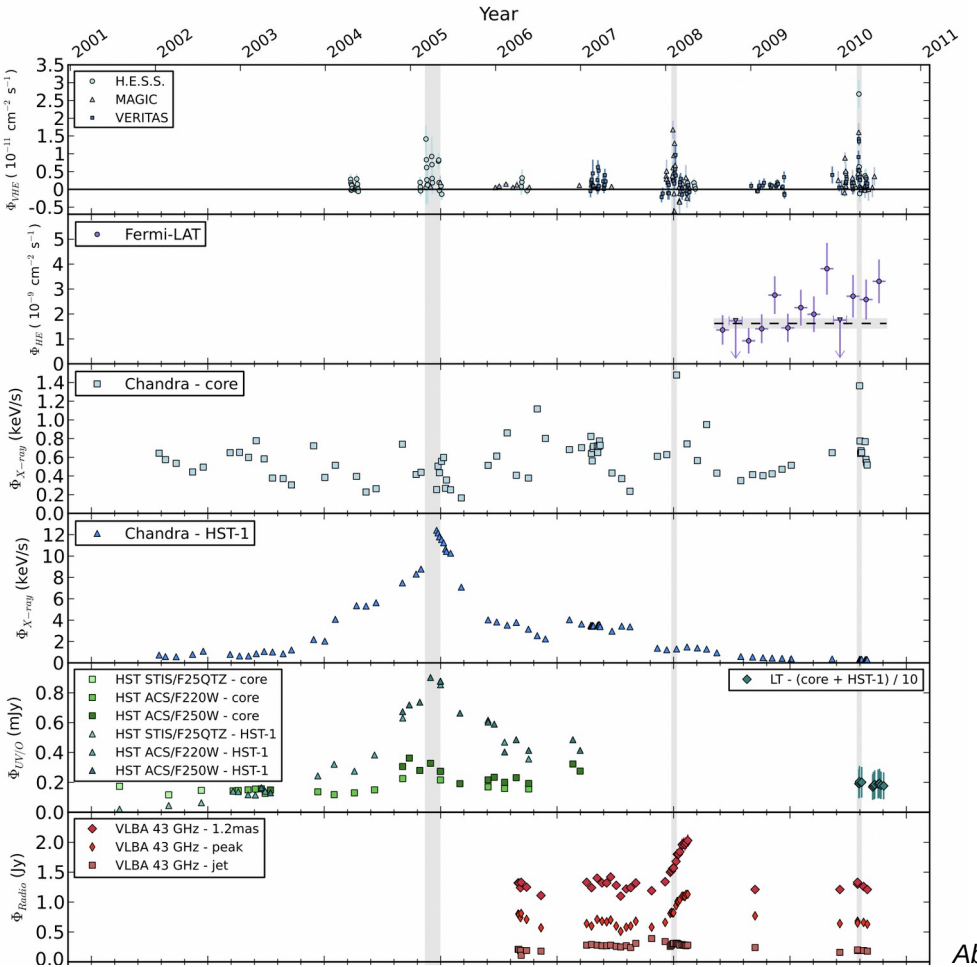

Abramowski. et al. 2012

BUT :

2005 VHE flare of the same source: Correlation with high activity (optical, X-rays) from the radio knot HST1.

Correlation of the 2010 VHE flares with the nucleus.

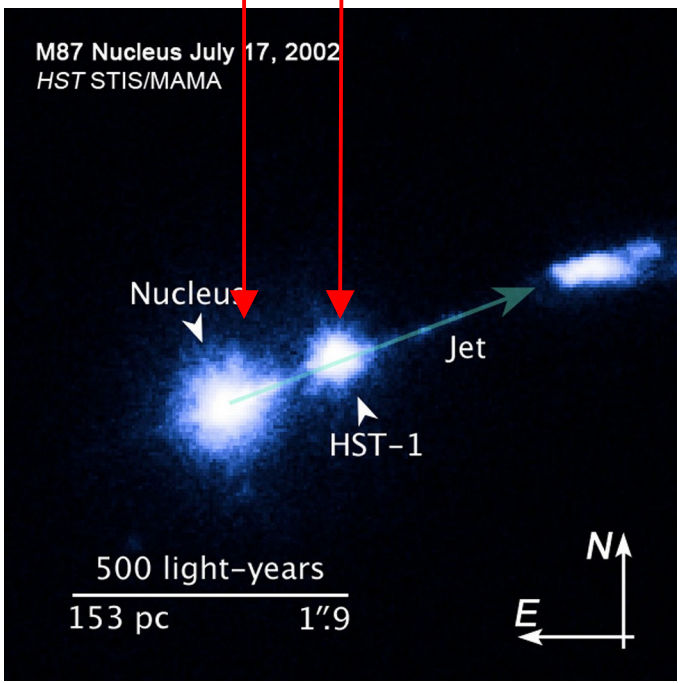

the VLBI – high-energy connection

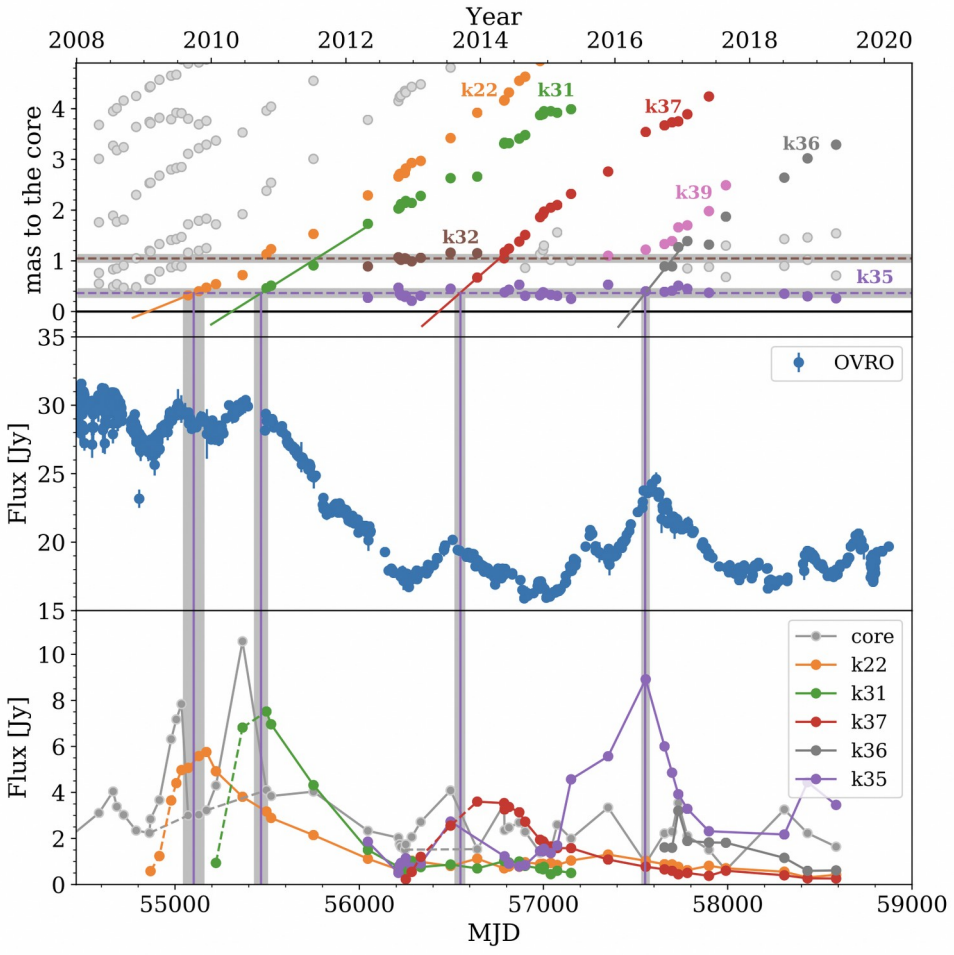

blazar 3C 273 observed at 15.3 GHz

upper panel : identification of moving and standing radio knots with the Mojave VLBI survey

middle panel : light curve of the overall radio flux from the jet

bottom panel : light curves of radio fluxes from individual knots

→ The crossing of moving knots through the position of standing knots coincides with flux increases in the moving knots. These are also visible in the overall emission, if they are isolated events.

→ Indication of **shock-shock interactions** inside the jet.

Fichet de Clairfontaine et al. (2020)

beyond the one-zone model

shock-shock interactions in an MHD jet

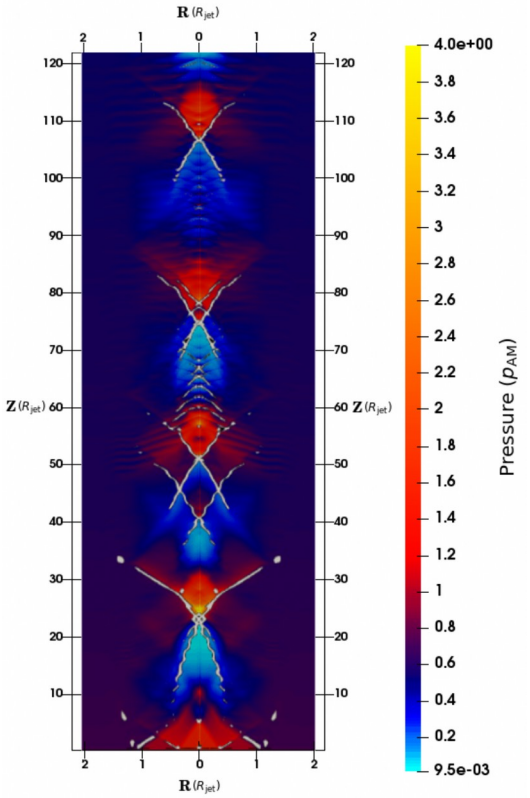

rarefaction (light blue) and compression (red) regions and associated standing shocks (white)

G. Fichet de Clairfontaine et al. 2021

In this example, an overpressured jet propagates in the ambient medium.

→ formation of a series of recollimation shocks (left)

A perturbation (= zone with elevated Lorentz factor or density) is injected at the base of the jet. A bow shock forms in front of the pertubation as it propagates through the jet.

→ shock-shock interactions lead to enhanced emission (i.e. flares), here observed in the radio band

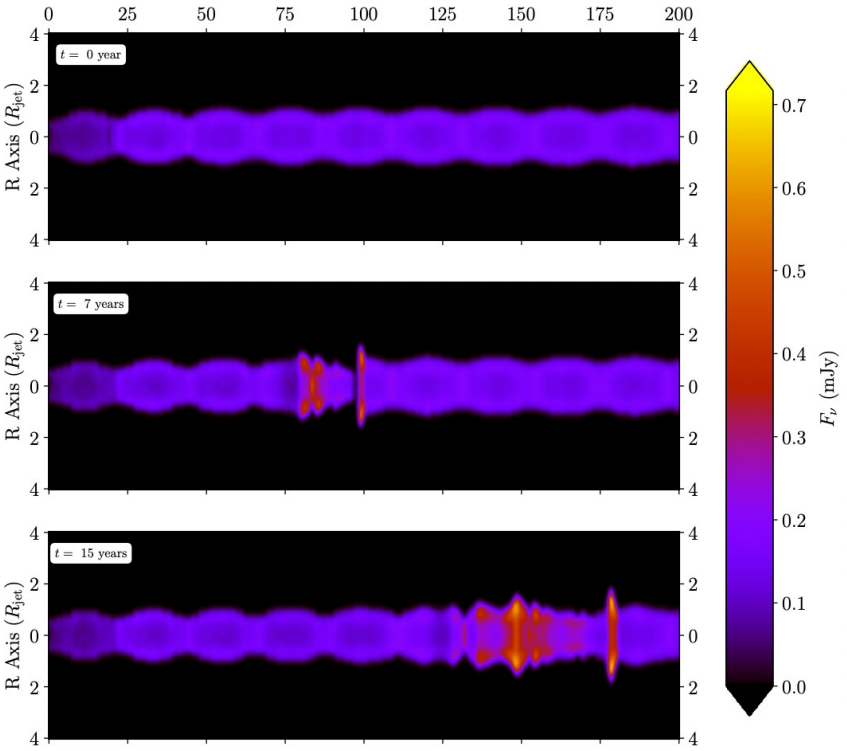

radio (synchrotron) emission from a perturbation crossing standing shocks

G. Fichet de Clairfontaine et al. 2022